HHS Public Access

Author manuscript

J Biol Rhythms. Author manuscript; available in PMC 2022 January 03.

Published in final edited form as:

J Biol Rhythms. 2021 April ; 36(2): 137–145. doi:10.1177/0748730420965285.

Photoreceptor degeneration in homozygous male Per2^{luc} mice during aging

Varunika Goyal[1,#], **Christopher DeVera**[1,#], **Kenkichi Baba**[1], **Jana Sellers**[2], **Micah A. Chrenek**[2], **P. Michael Iuvone**[2], **Gianluca Tosini**[1,2]

[1]Neuroscience institute and Department of Pharmacology & Toxicology, Morehouse School of Medicine, Atlanta, USA

[2]Department of Ophthalmology and Emory Eye Center, Emory University, Atlanta, Georgia, USA

Abstract

The Per2^{luc} mouse model developed by the Takahashi laboratory is one of the most powerful models to study circadian rhythms in real-time. In this study we report that photoreceptors degenerate in male Per2^{luc} mice during aging. Young (2.5-5 months - old) and aged (11-13.5 months-old) homozygous male Per2^{luc} mice and C57BL/6J mice were used for this study. Retina structure and function were investigated via spectral domain-optical coherence tomography (SD-OCT), fundus imaging, and electroretinography (ERG). Zonula occludens (ZO-1) immunofluorescence was used to analyze the retinal pigment epithelium (RPE) morphology (e.g., area, compactness, eccentricity, and solidity). Fundus examination revealed no difference between young Per2^{luc} and WT mice. However, the fundus of aged Per2^{luc} mice showed white deposits, suggestive of age-related drusen-like formation or microglia, which were absent in age-matched WT mice. No differences in retinal structure and function were observed between young Per2^{luc} and WT mice. However, with age Per2^{luc} mice showed a significant reduction in total retinal thickness with respect to C57BL/6J mice. The reduction was mostly confined to the photoreceptor layer. Consistent with these results, we observed a significant decrease in the amplitude of a- and b-waves of the ERG in aged Per2^{luc} mice. Analysis of the RPE morphology revealed that in aged Per2^{luc} mice there was an increase in compactness and eccentricity with a decrease in solidity with respect to the values observed in WT, pointing towards signs of aging in RPE of Per2^{luc} mice. Our data demonstrate that homozygous Per2^{luc} mice show photoreceptor degeneration during aging and a premature aging of the RPE. The mechanism responsible for this phenomenon is not known and needs to be further investigated.

Keywords

Per2luc; mice; photoreceptors; retinal pigment epithelium; circadian; aging

Corresponding author information: Name: Gianluca Tosini, PhD, **Mailing address:** 720 Westview Dr. SW, Atlanta, GA 30310, gtosini@msm.edu.

[#]equal contribution

Introduction

Circadian rhythms regulate key physiological functions in most organs and tissues (Takahashi, 2017). Several studies have also shown that these rhythms also contribute to the regulation of retinal functions (Felder-Schmittbuhl et al., 2018; DeVera et al., 2019) and photoreceptor viability during aging (Baba, et al., 2018a; Baba, et al., 2018b). Earlier investigations have demonstrated that the rodent's retina contains a circadian clock (Tosini & Menaker, 1996; Tosini & Menaker, 1998; Ruan et al., 2008). The understanding of the circadian organization of the mouse eye has been greatly facilitated by the use of the $Per2^{luc}$ mouse model developed by the Takahashi's laboratory (Yoo et al., 2004). Using $Per2^{luc}$ mice several studies have demonstrated that several tissues in the eye (e.g., retina, cornea and RPE) contain circadian clocks (Ruan et al., 2008; Baba et al., 2010; Jaeger et al., 2015; Baba et al., 2015). These studies have shown that circadian rhythms in the retina and retinal pigment epithelium (RPE) act independently from the master circadian clock located in the brain (Baba et al., 2010) and within the retina, the photoreceptor layer, the inner retinal layer and the ganglion cell layer all contain functional clocks that drive the circadian rhythm in $Per2^{luc}$ bioluminescence (Jaeger et al., 2015). The entrainment of these circadian clocks is probably mediated by dopamine via dopamine 2 receptors in the RPE (Baba et al., 2017), dopamine 1 receptors in the retina (Ruan et al., 2008) and by melatonin, via melatonin receptors type 2, in the cornea (Baba et al., 2015). Additional studies have also shown that rod photoreceptors (Calligaro et al., 2019) and ganglion cells expressing OPN5 (Buhr et al., 2015) are responsible for the entrainment of the retinal circadian rhythm.

During the course of these studies on the circadian organization of the mouse retina, we noticed older homozygous $Per2^{luc}$ mice showed a more pronounced decrease in amplitude of the a and b-wave of the electroretinogram (ERG) than age matched C57BL/6J mice, thus suggesting the possibility that the insertion of the $Per2^{luc}$ construct may have a negative effect on retinal cells.

Materials and Methods

Animals

Male C57BL/6J (Jackson laboratory, 000664) and male homozygous $Per2^{luc}$ (Yoo et al., 2004; with an in-frame fusion of firefly luciferase to Per2, and an SV40 polyadenylation signal; JAX laboratory - 006852) were maintained and bred for 50 generations at Morehouse School of Medicine. Mice were maintained under a 12:12 light:dark cycle (300-400 Lux during the light phase) and food and water access was *ad libitum*. Verification of homozygous $Per2^{luc}$ genotype was done as described (Yoo et al., 2004). $Per2^{luc}$ mice were also genotyped to verify the absence of known mutations like *rd1* (5'-TAGCCCCAAGCACCTATCTA-3' and 5'-TGTGCATGTTGGATGTTTTT-3') and *rd8* (Mattapallil et al., 2012) that affect photoreceptor health. The age of all the mice used in following analysis has also been in days in the supplemental file (Table S1.)

Spectral Domain-Optical Coherence Tomography (SD-OCT)

Per2^{luc} and C57BL/6J mice were analyzed for retinal structure by using a Micron IV SD-OCT system and a fundus camera (Phoenix Research Labs, Pleasanton, CA) as previously described (Goyal et al., 2020) at ZT6. Briefly, mice were anesthetized with ketamine/xylazine cocktail and kept on Micron IV SD-OCT platform. SD-OCT images were obtained from the left and right eyes after a sharp and clear image of the fundus (with the optic nerve centered) was obtained. SD-OCT was a circular scan about 100 μm from the optic nerve head. Fifty scans from each eye were averaged. The retinal layers (indicated on the figure images) were identified according to published nomenclature. Total retinal thickness and thickness of the individual retinal layers were analyzed by using NIH Image J (1.51w).

Electroretinogram (ERG)

Per2^{luc} and C57BL/6J mice were dark-adapted for at least 1 hour starting ZT5 – ZT6 and anesthetized with ketamine/xylazine mixture. All preparation of ERG recordings was conducted under dim red light (<3 lux, 15W Kodak safe lamp filter 1A, Eastman Kodak, Rochester, NY, USA) as previously described (Goyal et al., 2020) measuring ERG responses at ZT6 - ZT7. Briefly, mouse eyes were presented with seven series of flash intensity between from 0.03 to 6.28 cd*s/m^2 with intervals of flashes from 0.612 to 30 seconds. For light-adapted responses (photopic), cone-associated activity was isolated by over-saturating rods with 63 cd*s/m^2 of steady white background light. A series of four consecutive white flashes (79.06 cd*s/m^2) were introduced at 2.5 min, 5 min, 10 min, and 15 min during the background light exposure. The traces of the ERG were averaged and stored on a computer for later analysis. Amplitude of the b-wave was measured from the trough of the a-wave to the peak of the b-wave or from the baseline to the b-wave peak, in case a-wave was not present.

RPE morphology analysis

Whole eyes from C57BL/6J and Per2^{luc} mice, were enucleated, processed, and immunostained as previously described (Goyal et al., 2020) at ZT6. Briefly, each eye following enucleation was placed in Z-fix (Anatech, 170) for 10 minutes at room temperature and then rinsed up to five times with 0.01 M phosphate buffered saline. On a clean microscope slide (VWR, 16004-406), radial cuts around the limbus of the eye were made using spring scissors (WPI, 501235) to remove the anterior segment of the eye (cornea and lens). The remaining eye cup was divided into 4 petals and allowed to be flattened against the microscope slide. The now exposed retina was peeled by using Dumont #5/45 forceps (FST, 11251-35) and RPE flat mounts were placed in a 24 well plate (Fisher, 12565501) with 0.01 M phosphate buffered saline and processed immediately for zonula occludens-1 (ZO-1) immunostaining. RPE flat mounts were blocked and then incubated with ZO-1 antibody (1:500, Millipore Sigma, MABT11) overnight at 4°C. Flat mounts were washed and incubated in Alexa Fluor 488 (1:500, goat anti-rat, Invitrogen, A110006) for up to 2 hours on a shaker at room temperature. RPE cell junctions were visualized on a confocal microscope (Zeiss LSM 700) in the 488 nm channel, and autofluorescent particles were visualized in the 568 nm channel. In order to determine the number of autofluorescent particles per RPE cell, a pipeline in Cell Profiler (v 2.2.0) was created to:

1) identify RPE cells on the isolated RPE flat mount via ZO-1 staining, 2) identify all autofluorescent particles present on the RPE flat mount, 3) create a mask from the ZO-1 labeling to identify RPE cells, and 4) count the number of autofluorescent particles in each RPE cell. Additionally, RPE cell morphology parameters such as area, eccentricity, solidity, and compactness were measured from step 1 on isolated RPE cells, as previously described (Boatright et al., 2015; Supplemental file S2). For all RPE morphology analyses, only central measurements were made on each RPE petal (up to 1.0 mm from the optic nerve head).

Statistical Analysis

Data were analyzed with t-test or two-way ANOVA. Post hoc multiple comparisons of interactions were performed with the Tukey's test (GraphPad Prism). Significance level was set at $P = 0.05$ with a power >0.8. Data are expressed as mean ± standard error of the mean (SEM).

Results

Aging induces a decrease in the photoreceptor layer thickness and functioning in Per2^{luc}

The total retinal thickness and the thickness of different retinal layers were not different between young C57BL/6J and Per2^{luc} mice (Fig. 1A; *t*-test, $p > 0.05$ in both cases). A significant reduction in total retinal thickness was observed in the older Per2^{luc} mice with respect to age-matched C57BL/6J (Fig. 1B; t-test, $p < 0.05$). Among the different retinal layers, the reduction in the thickness was most pronounced in the outer nuclear layer and photoreceptor layer of the Per2^{luc} mice (Fig. 1 C, D; two-way ANOVA; Tukey post-hoc, $p < 0.05$).

Consistently with these results, we did not observe any significant differences in a- and b-wave amplitude of the scotopic ERGs between the two genotypes at the younger age (Fig. 2; two-way ANOVA, $p > 0.05$) whereas a significant reduction in a- and b-wave amplitude of the scotopic ERG was observed in older Per2^{luc} with respect to age-matched C57BL/6J (Fig. 2; two-way ANOVA, Tukey post-hoc, $p < 0.05$).

Interestingly the photopic ERGs did not overtly differ between the two genotypes at both ages investigated (Fig. 2; two-way ANOVA, Tukey post-hoc, $p < 0.05$), thus suggesting that cone photoreceptors functioning is not affected by aging in Per2^{luc} mice.

Increased non-RPE specific autofluorescence in old Per2^{luc} mice eyes.— Fundus analysis of the eyes for both C57BL/6J and Per2^{luc} mice at younger age did not exhibit any obvious fundus autofluorescence (Fig. 3). However, in old mice, there was an obvious visual difference in the fundus of aged Per2^{luc} mice when compared to aged C57BL/6J (Fig. 3). Using cell profiler, we then measured the total number of apical autofluorescent particles present in isolated RPE cells on a flat mount preparation (Fig 3) in C57BL/6J and Per2^{luc} mice at young and old age. No difference in the total number of apical autofluorescent particles of isolated RPE cells was observed in an RPE flat mount preparation from C57BL/6J or Per2^{luc} mice (Fig 3, $p > 0.05$, two-way ANOVA, Tukey post-hoc).

Aged Per2^{luc} RPE cells exhibited altered morphology parameters

No differences in compactness, eccentricity, and solidity were observed in younger C57BL/6J and Per2^{luc} RPE cells (Fig 4, $p > 0.05$, two-way ANOVA). However, there was a slight increase in total RPE cell area in Per2^{luc} mice compared to C57BL/6J (Fig. 4; $p < 0.05$, two-way ANOVA; Tukey post-hoc). In the older Per2^{luc} mice we observed an increase in compactness and eccentricity (Fig. 4, $p < 0.05$, two-way ANOVA; Tukey post-hoc) and a decrease in solidity when compared to age matched C57BL/6J mice (Fig. 4; $p < 0.05$, two-way ANOVA; Tukey post-hoc).

Discussion

The use of the Per2^{luc} mouse has been an invaluable tool to dissect the mouse circadian system and we are not aware of any other study that has shown negative effect of this genetic manipulation. The data reported in this study indicate that aged male homozygous Per2^{luc} mice show the following phenotypes: *i*) total retina thickness is decreased in Per2^{luc} mice during old age with respect to age matched controls; *ii*) this decrease is almost exclusively attributed to reduction in the thickness of the photoreceptor layer; and *iii*) the RPE of aged Per2^{luc} mice showed clear signs of premature aging.

The photoreceptor layer of the mouse retina is mostly constituted by the rod photoreceptors since cones represent only 3% of the photoreceptors (Jeon et al. 1998). Hence the significant decrease observed in the thickness of photoreceptor layer thickness (about 25%) suggests that rod photoreceptor viability is reduced during the aging process in Per2^{luc} mice. The ERG data further support this finding since only the scotopic ERG (i.e., the response of the rods) is affected in old Per2^{luc} whereas the photopic ERG (i.e., the response of the cones) does not appear to have major deficits in aged Per2^{luc} mice. It is also worth noting that the other retinal layers did not shown any changes, at least as assessed by SD-OCT.

Our data also show that the RPE of the Per2^{luc} mice may show signs of premature aging as indicated by the increase of putative basal autofluorescence bodies present in the fundus image (Figure 3) and in the morphological analysis of the RPE cells (Figure 4). The fact that no significant differences were found in the analysis of the autofluorescence of the apical surface of the RPE cells (Figure 3) while there were obvious difference in the fundus autofluorescence, can be explained by the fact that the source of fundus autofluorescence observed with fundus imaging is located between the basal surface of the RPE and Bruch's membrane (see review: Sparrow and Duncker, 2014).

Previous studies have shown that within the retina many cell types (e.g., ganglion, bipolar, amacrine, etc.,) contain circadian clocks, but the rod photoreceptors are believed to lack the molecular machinery necessary to generate circadian oscillation (Ruan et al., 2006; Liu et al., 2012). Additional studies have suggested that within the photoreceptor layer only cones seem to harbor a circadian clock (Storch et al., 2007; Liu et al., 2012; Baba, Piano, et al., 2018). Thus, it is puzzling that the negative effects of Per2^{luc} are observed in a cell type that probably does not contain a functional circadian clock. On the other hand, the RPE - which contains a functional circadian clock (Baba et al., 2010; Baba et al., 2017) - also showed premature aging in Per2^{luc} homozygous mice. Since the retina and RPE are tightly

connected and the health of one depends from the health status of the other (Sparrow et al., 2010), it is plausible to speculate that the reduction of the rod photoreceptors may be a consequence of the RPE premature aging in the presence of the Per2^{luc} construct in these cells.

It is worth noting that in our study we have used mice homozygous for the Per2^{luc} whereas the vast majority of the other studies have used Per2^{luc} heterozygous mice. Although we have not performed a systematic analysis, it is worthwhile here to mention is that in a preliminary study using mice heterozygous for Per2^{luc} mice, we did not observe any negative retinal phenotype. Thus, we believe that the negative effects observed in our study are only present in homozygous Per2^{luc} and we suggest – that at least for aging studies – not using Per2^{luc} homozygous mice.

It important here to mention that the underlying molecular mechanism responsible for the observed phenomenon is unknown. However, we believe that the effects do not involve dysfunction of the molecular clockwork since other cell types in retina that are known contain a circadian clock were unaffected. Furthermore, homozygous Per2^{luc} mice do not show any difference in the entrainment to L:D cycle, free running period, amplitude of circadian rhythms, activity levels, and phase-shifts with respect to C57BL/6J mice or to Per2^{luc} heterozygous mice (Yoo et al., 2004). Therefore, we believe that the identification of the possible mechanism will require a sophisticated analysis at the genomic and proteomic levels, which are beyond the scope of the present study. Finally, it is worth mentioning that in our study we only used male mice and thus it is possible – although we do not believe likely - that female Per2^{luc} homozygous mice may not show the same phenotype that we have observed in male Per2^{luc} homozygous mice. In conclusion, our studies have shown that male homozygous Per2^{luc} mice show a significant decrease in the thickness of photoreceptor layer and premature aging of the RPE. However, the mechanisms responsible for such effects are not known and such understanding will require additional studies focusing on the molecular mechanisms.

Supplementary Material

Refer to Web version on PubMed Central for supplementary material.

Acknowledgments:

This work was supported by National Institutes of Health Grants: GM116760 to K.B.; EY026291to G.T. and NS083932 to Morehouse School of Medicine; EY004864, EY027711, and EY006360 to P.M.I.; and an unrestricted departmental grant from Research to Prevent Blindness (Emory Department of Ophthalmology).

References

Baba K, Davidson AJ, Tosini G (2015) Melatonin Entrains Per2^{luc} Bioluminescence Circadian Rhythm in the Mouse Cornea. Invest Ophthalmol Vis Sci. 56(8):4753–4758. [PubMed: 26207312]

Baba K, DeBruyne JP, Tosini G (2017) Dopamine 2 Receptor Activation Entrains Circadian Clocks in Mouse Retinal Pigment Epithelium. Sci Rep. 7(5103):1–7. [PubMed: 28127051]

Baba K, Piano I, Lyuboslavsky P, Chrenek MA, Sellers JT, Zhang S, Gargini C, He L, Tosini G, Iuvone PM (2018a) Removal of clock gene Bmal1 from the retina affects retinal development and accelerates cone photoreceptor degeneration during aging. Proc Natl Acad Sci.:201808137.

Baba K, Ribelayga CP, Iuvone PM, Tosini G (2018b) The Retinal Circadian Clock and Photoreceptor Viability. Adv Exp Med Biol. 1074:345–350. [PubMed: 29721962]

Baba K, Sengupta A, Tosini M, Contreras-Alcantara S, Tosini G (2010) Circadian regulation of the PERIOD 2::LUCIFERASE bioluminescence rhythm in the mouse retinal pigment epithelium-choroid. Mol Vis. 16:2605–2611. [PubMed: 21151601]

Boatright JH, Dalal N, Chrenek MA, Gardner C, Ziesel A, Jiang Y, Grossniklaus E, Nickerson JM (2015) Methodologies for analysis of patterning in the mouse RPE sheet. Mol Vis. 21:40–60 [PubMed: 25593512]

Buhr ED, Yue WWS, Ren X, Jiang Z, Liao H-WR, Mei X, Vemaraju S, Nguyen M-T, Reed RR, Lang RA, Yau K-W, Gelder RNV (2015) Neuropsin (OPN5)-mediated photoentrainment of local circadian oscillators in mammalian retina and cornea. Proc Natl Acad Sci. 112(42):13093–13098. [PubMed: 26392540]

Calligaro H, Coutanson C, Najjar RP, Mazzaro N, Cooper HM, Haddjeri N, Felder-Schmittbuhl M-P, Dkhissi-Benyahya O (2019) Rods contribute to the light-induced phase shift of the retinal clock in mammals. PLOS Biol. 17(3):e2006211. [PubMed: 30822304]

DeVera C, Baba K, Tosini G (2019) Retinal Circadian Clocks are Major Players in the Modulation of Retinal Functions and Photoreceptor Viability. Yale J Biol Med. 92:233–240. [PubMed: 31249484]

Felder-Schmittbuhl M-P, Buhr ED, Dkhissi-Benyahya O, Hicks D, Peirson N, Ribelayga CP, Sandu C, Spessert R, Tosini G (2018) Ocular Clocks: Adapting Mechanisms for Eye Functions and Health. Invest Ophthalmol Vis Sci. 59(12):4856–4870. [PubMed: 30347082]

Goyal V, DeVera C, Laurent V, Sellers J, Chrenek MA, Hicks D, Baba K, Iuvone PM, Tosini G (2020) Dopamine 2 Receptor Signaling Controls the Daily Burst in Phagocytic Activity in the Mouse Retinal Pigment Epithelium. Invest Ophthalmol Vis Sci. 61(5):10–10.

Jaeger C, Sandu C, Malan A, Mellac K, Hicks D, Felder-Schmittbuhl M-P (2015) Circadian organization of the rodent retina involves strongly coupled, layer-specific oscillators. FASEB J. 29(4):1493–1504. [PubMed: 25573753]

Jeon C-J, Strettoi E, Masland RH (1998) The Major Cell Populations of the Mouse Retina. J Neurosci. 18(21):8936. [PubMed: 9786999]

Liu X, Zhang Z, Ribelayga CP (2012) Heterogeneous Expression of the Core Circadian Clock Proteins among Neuronal Cell Types in Mouse Retina. PLOS ONE. 7(11):e50602. [PubMed: 23189207]

Mattapallil MJ, Wawrousek EF, Chan CC, Zhao H, Roychoudhury J, Ferguson TA, & Caspi RR (2012). The Rd8 mutation of the Crb1 gene is present in vendor lines of C57BL/6N mice and embryonic stem cells and confounds ocular induced mutant phenotypes. Invest Ophthal Vis Sci. 53(6), 2921–2927. [PubMed: 22447858]

Ruan G-X, Allen GC, Yamazaki S, McMahon DG (2008) An Autonomous Circadian Clock in the Inner Mouse Retina Regulated by Dopamine and GABA. PLOS Biol. 6(10):e249. [PubMed: 18959477]

Ruan G-X, Zhang D-Q, Zhou T, Yamazaki S, McMahon DG (2006) Circadian organization of the mammalian retina. Proc Natl Acad Sci. 103(25):9703–9708. [PubMed: 16766660]

Sparrow J and Dunker T (2014). Fundus Autofluorescence and RPE Lipofuscin in Age-Related Macular Degeneration. J Clin Med. 3(4): 1302–1321. [PubMed: 25774313]

Sparrow J, Hicks D, Hamel CP (2010) The Retinal Pigment Epithelium in Health and Disease. Curr Mol Med. 10(9):802–823. [PubMed: 21091424]

Storch K-F, Paz C, Signorovitch J, Raviola E, Pawlyk B, Li T, Weitz CJ (2007) Intrinsic circadian clock of the mammalian retina: importance for retinal processing of visual information. Cell. 130(4):730–741. [PubMed: 17719549]

Takahashi JS (2017) Transcriptional architecture of the mammalian circadian clock. Nat Rev Genet. 18(3):164–179. [PubMed: 27990019]

Tosini G, Menaker M (1996) Circadian Rhythms in Cultured Mammalian Retina. Science. 272(5260):419–421. [PubMed: 8602533]

Tosini G, Menaker M (1998) The clock in the mouse retina: melatonin synthesis and photoreceptor degeneration. Brain Res. 789(2):221–228. [PubMed: 9573370]

Yoo S-H, Yamazaki S, Lowrey PL, Shimomura K, Ko CH, Buhr ED, Siepka SM, Hong H-K, Oh WJ, Yoo OJ, Menaker M, Takahashi JS (2004) PERIOD2::LUCIFERASE real-time reporting of

circadian dynamics reveals persistent circadian oscillations in mouse peripheral tissues. Proc Natl Acad Sci. 101(15):5339–5346. [PubMed: 14963227]

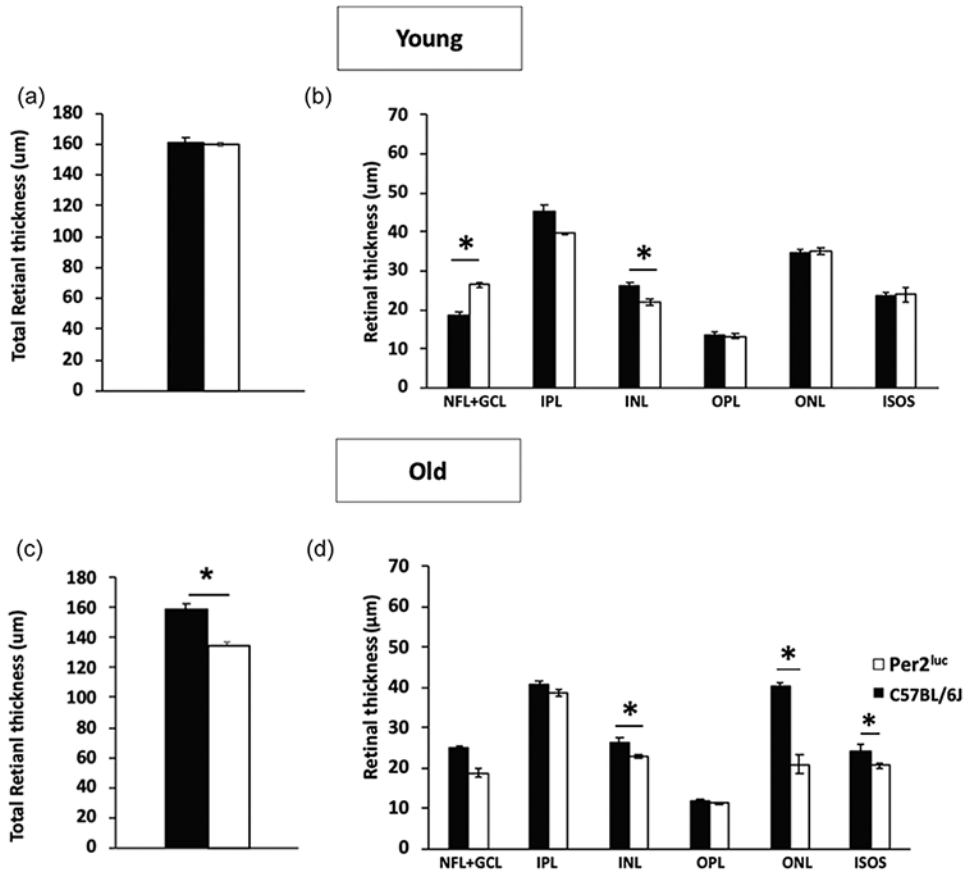

Figure 1. Per2^{luc} mice show a significant reduction in the photoreceptor layer thickness during aging.

Measurement of *in vivo* retinal thickness in both C57BL/6J and Per2^{luc} mice revealed no differences in total retinal thickness in the young (A; $p > 0.05$, t-tests; n=5-6). When we measure the thickness of the different retinal layers, a small difference was observed in the NFL-GCL and in the INL (C; $p > 0.05$, two-way ANOVA, Tukey post-hoc, n=5-6) at 3 months of age. However, at 12 months of age, there was a significant decrease in the total retinal thickness in Per2^{luc} mice when compared to age matched C57BL/6J mice (B; *=$p < 0.05$, t-test, n=5-6). A small decrease in the thickness of INL was detected in older Per2^{luc} mice (D; *=$p < 0.05$, two-way ANOVA, Tukey post-hoc) and a much more pronounced reduction was observed in the photoreceptor layer (ONL and ISOS) was observed in aged Per2^{luc} mice (D; *=$p < 0.05$, two-way ANOVA, Tukey post-hoc). No significant differences were detected in the other retinal ($p > 0.05$, two-way ANOVA). NFL- Nerve fiber layer; GCL- Ganglionic cell layer; IPL-Inner Plexiform layer; OPL- Outer plexiform layer, ONL-Outer Plexiform layer, ISOS- Inner segment and outer segment (n=5-6 in all cases).

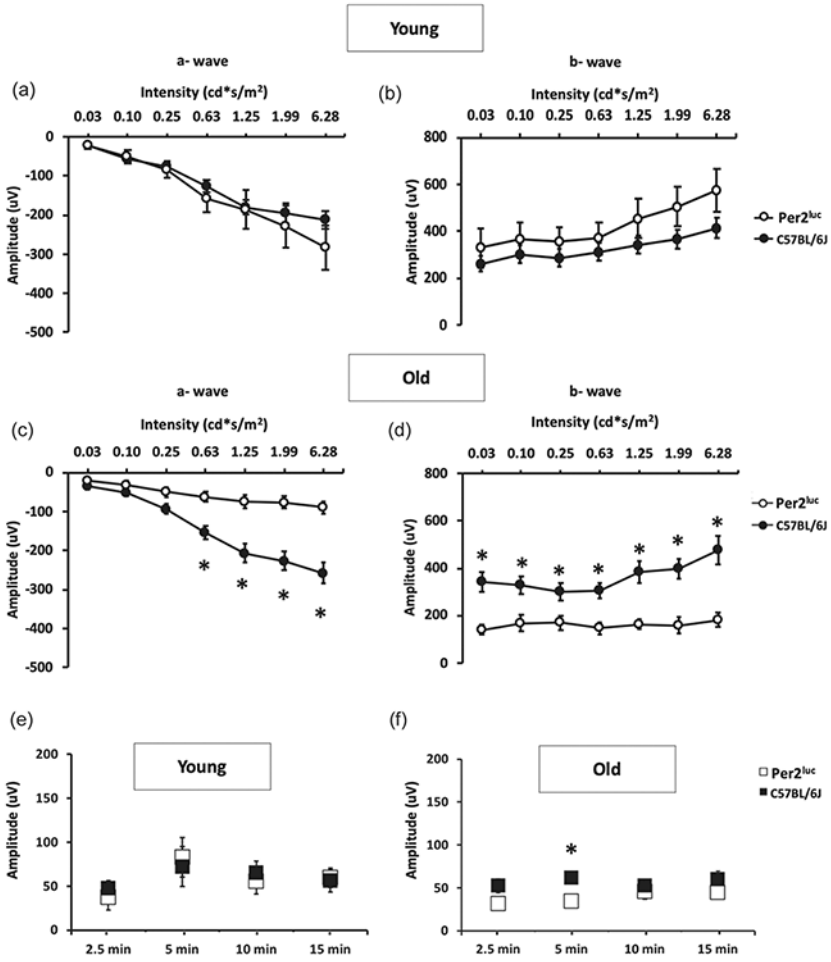

Figure 2. The amplitude of a and b-wave of the scotopic ERG is reduced in aged Per2^{luc} mice.

Assessing photoreceptor function for C57BL/6J and Per2^{luc} mice revealed no difference in scotopic a-wave (A; $p > 0.05$, two-way ANOVA, Tukey post-hoc, n=5-6) or b-wave (B; $p > 0.05$, two-way ANOVA, Tukey post-hoc, n=5-6) at the younger age. However, with aging, Per2^{luc} mice exhibited decreased photoreceptor function in both the a-wave (C; *= $p < 0.05$, two-way ANOVA, Tukey post-hoc, n=5-6) and b-wave (D; *=$p < 0.05$, two-way ANOVA, Tukey post-hoc, n=5-6) when compared to similarly aged C57BL/6J mice. Interestingly, the photopic response of both young (E; $p > 0.05$, two-way ANOVA, Tukey post-hoc, n=5-8) and old mice (F *=$p < 0.05$, two-way ANOVA, tukey post-hoc, n=5-8) had similar cone photoreceptor response in Per2^{luc} when compared to similarly aged C57BL/6J mice.

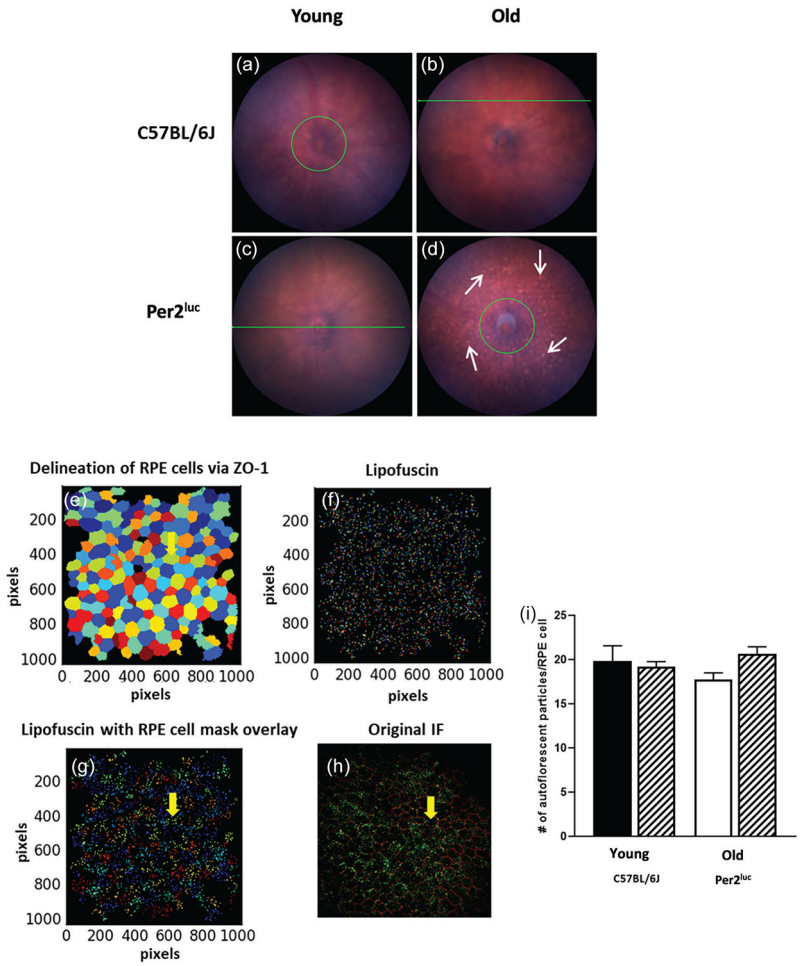

Figure 3. Aged Per2^{luc} mice display some abnormality in the fundus, but no difference in RPE cell apical autofluorescence.

At the younger age, no differences were observed in the fundus image between the two genotypes (A, B) whereas at older age we observed an increase in the number of fundus autofluorescence spots (white arrows) in Per2^{luc} (D) when compared to C57BL/6J of similar age (C). We then counted the number of apical autofluorescent particles present in isolated RPE cells in RPE flat mount preparation using cell profiler (v 2.2.0) which allowed the delineation of RPE cells via ZO-1 staining (E) and autofluorescent particles (i.e., lipofuscin) (F). Finally an RPE cells ZO-1 mask was created which was then overlaid on the isolated autofluorescent particles (G). When the lipofuscin particles were counted in each isolated RPE cell, there were no differences observed in the number of autofluorescence particles (I; $p > 0.05$, two-way ANOVA, Tukey post-hoc, n=3-4). A representative immunofluorescence image of a typical RPE flat mount with ZO-1 and autofluorescent particles from a young C57BL/6J mouse (H).

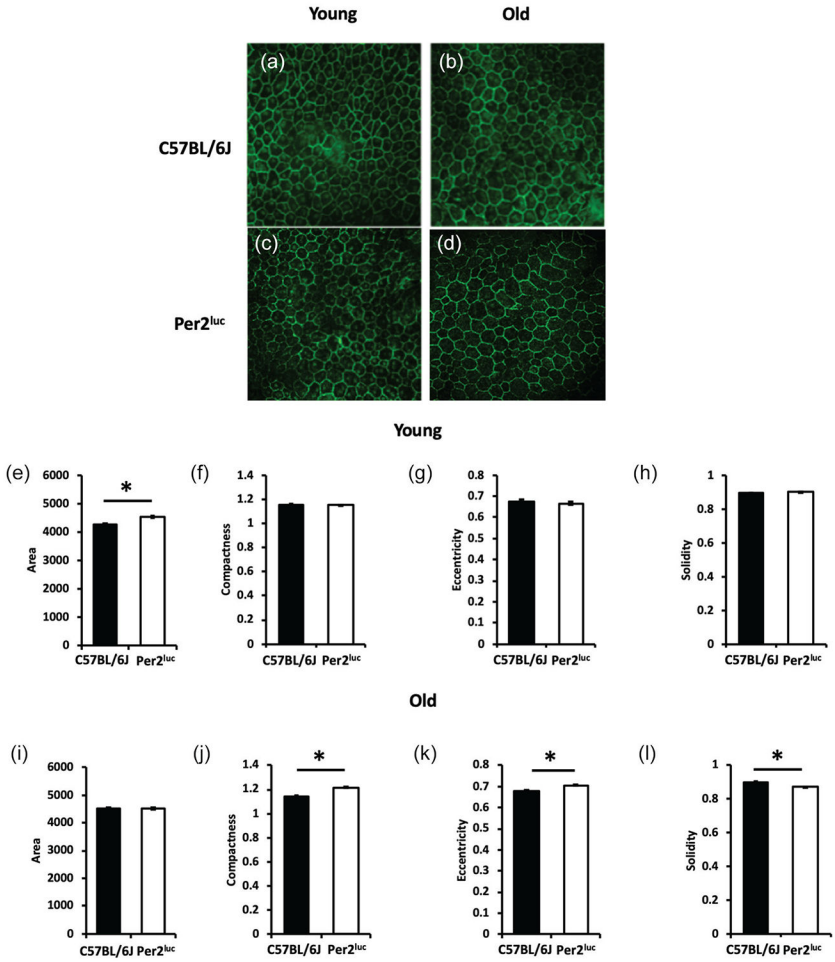

Figure 4. Aged Per2^{luc} mice show signs of premature aging in the RPE.

RPE cell shape morphology was assessed in young C57BL/6J (A) and Per2^{luc} (C) mice and old C57BL/6J (B) and Per2^{luc} (D). We observed an increase in total RPE cell area in young Per2^{luc} mice when compared to similarly aged C57BL/6J mice (E; *=$p < 0.05$, two-way ANOVA, Tukey post-hoc, n=3-4) with no change in the other cell morphology parameters measured at this age (F, G, H; $p > 0.05$, two-way ANOVA, n=3-4). However, when these mice were old, there was no longer any difference in total RPE cell area (I; $p > 0.05$, two-way ANOVA, n=3-4) but there was an increase in compactness, eccentricity, and a decrease in solidity when compared to age-matched C57BL/6J mice (J, K, L; *=$p < 0.05$, two-way ANOVA, Tukey post-hoc, n=3-4). Photomicrographs show representative RPE flat mount images of ZO-1 cell junction protein demarcating RPE cell boundaries in C57BL/6J and Per2^{luc} mice at both young and old age.